

Research Article

Numerical Study on the Disturbance Effect of Short-Distance Parallel Shield Tunnelling Undercrossing Existing Tunnels

Zhen Huang,¹ Chenlong Zhang,¹ Helin Fu,² Huangshi Deng ,² Shaokun Ma ,¹ and Jiajun Fu³

¹College of Civil Engineering and Architecture, Key Laboratory of Disaster Prevention and Structural Safety, Guangxi University, Nanning 530004, China

²School of Civil Engineering, National Engineering Laboratory for Construction Technology of High Speed Railway, Central South University, Changsha 410075, China

³School of Computing, Beijing University of Post and Telecommunication, Beijing 100876, China

Correspondence should be addressed to Huangshi Deng; tunneldhs@csu.edu.cn and Shaokun Ma; mashaokun@sina.com

Received 3 June 2020; Revised 29 August 2020; Accepted 10 September 2020; Published 21 September 2020

Academic Editor: Chunshun Zhang

Copyright © 2020 Zhen Huang et al. This is an open access article distributed under the Creative Commons Attribution License, which permits unrestricted use, distribution, and reproduction in any medium, provided the original work is properly cited.

The construction of new tunnels poses a threat to the operational safety of closely existing tunnels, and the construction mode of parallel undercrossing over short distances has the most significant impact. In this study, a new double-line shield tunnel parallel undercrossing of existing tunnels in Hefei, China, is taken as an example. A three-dimensional (3D) numerical model using FLAC^{3D} finite difference software was established. The dynamic construction of the new double-line shield tunnel undercrossing the existing subway tunnel over a short distance and in parallel was simulated. The pattern of existing tunnel settlement and change in lining stress caused by the shield tunnelling process were analyzed. The reliability of simulation was verified through field-monitoring data. Finally, based on the numerical model, the effects of change in stratum sensitivity on the settlement of existing tunnel, lining internal force, and surface settlement are discussed. The results show that during shield tunnelling, the maximum ground settlement is 3.9 mm, the maximum settlement at the arch waist of existing tunnel near the new tunnel is 7.75 mm, and the maximum vault settlement is 5.38 mm. The maximum stress of lining of existing tunnel before the excavation is 7.798×10^5 Pa. After the construction of double-line shield tunnel, the maximum stress of lining is 1.124×10^6 Pa, an increase of 44% than that before the construction. The surface settlement and tunnel settlement are sensitive to the weakening of soil layer strength, and lining stress is not affected by the weakening of soil layer strength. The field-monitoring results are consistent with the numerical simulation results, and the model calculation is reliable. This study plays an important role in ensuring construction safety and optimizing the construction risk control of a tunnel.

1. Introduction

In China, subway transportation has shown a leap forward in development, especially in some large cities. Subway lines have gradually developed into a network and three-dimensional (3D) form. The 3D construction is mainly reflected in the 3D intersection of tunnel space, easily causing disturbance and damage to existing tunnels [1]. According to the relative position relationship between a new tunnel and existing tunnel, the undercrossing construction is mainly divided into three modes: orthogonal, oblique, and

parallel. According to relevant studies, the construction mode of close parallel undercrossing has the greatest effect on the disturbance of existing tunnels and the highest construction risk [2, 3]. Therefore, to ensure the safety and stability of an existing tunnel, it is necessary to conduct safety analysis before construction to develop a strict construction control scheme.

The construction of an urban subway tunnel inevitably affects the existing structure around it (e.g., tunnels, pipes, and buildings). An undercrossing tunnel changes the balanced stress field and induces settlement, resulting in an

additional load and bending moment on the existing structure and further threatening its normal operation [2, 4]. Many empirical or semiempirical methods, physical model experiments, analytical methods, and numerical methods have been used to study the effect of adjacent tunnel construction on the existing structure. While the effect of adjacent tunnelling on existing buildings [5, 6], roads [7], pipelines [8, 9, 10], or bridges [11] has been extensively studied using the aforementioned methods, the effects of undercrossing tunnelling on existing tunnels have been less studied [4].

Empirical or semiempirical methods have simple and practical characteristics, and they are widely used in practice. For example, based on monitoring data, Fang et al. [12] used an empirical method to study the settlement of a tunnel crossing two existing tunnels to solve the settlement problem of the existing tunnel. Chen et al. [13] studied the deformation and stress characteristics of an existing tunnel caused by a closed earth pressure balance (EPB) shield during an oblique crossing process. The Gauss distribution curve of displacement was used to simulate the settlement profile of existing tunnel. Physical model tests include scale model tests and centrifugal model tests. The tests truly reflect the field situations, but this method has high cost and a long test cycle. Through large-scale model tests, Byun et al. [14] studied the surface characteristics and tunnel behavior of existing tunnels above and below newly excavated tunnels. The results show that the existence of an upper tunnel significantly affects the stress flow produced by the longitudinal arching effect of lower tunnel excavation. The analytical method is to analyze the effect of mechanical behavior of tunnel construction by simplifying the constitutive behavior of soil (elastic or elastoplastic). For example, based on *in situ* monitoring data, Zhang and Huang [15] presented an analytical solution to calculate the deformation of existing subway tunnels induced by an EPB shield during above-overlapped and down-overlapped crossing tunnels with oblique angles. Liang et al. [2] proposed an analytical method to analyze the deformation of an existing tunnel caused by crossing over a new tunnel, and based on the Winkler foundation model, the interaction between tunnel and soil caused by unloading stress was analyzed. Numerical simulation methods such as finite element method (FEM) or finite difference method (FDM) not only consider the heterogeneity and nonlinear characteristics of soil but also truly describe the complex geometry and dynamic construction process. These are the most economical methods widely used to study the interaction between new and existing tunnels. For example, Lin et al. [16] used a numerical simulation method to simulate the deformation characteristics of a new double tunnel obliquely crossing an existing tunnel. Through 3D numerical analysis, Ng et al. [17] studied the effects of ratio of breadth of an existing horseshoe-shaped tunnel to the diameter of new circular tunnels on the interaction of perpendicularly crossing tunnels in sand. Yin et al. [18] built a 3D finite element numerical model and analyzed the deformation of existing tunnels induced by the construction of new vertical undercrossing tunnels.

With the development of underground space and improvement in space utilization rates, the number of close parallel undercrossing projects will increase. However, in previous studies, the new tunnel construction mode of undercrossing mainly focused on orthogonal and oblique modes, while the construction mode of close parallel undercrossing was rarely studied. In fact, the effect of parallel undercrossing of new double-track tunnels on the disturbance of existing tunnels may be greater than that of orthogonal or oblique undercrossing. Parallel undercrossing has a long disturbance distance and space-time effect, which might lead to 3D changes in the settlement and deformation of existing tunnels and endanger the operational safety of existing tunnels. Therefore, it is necessary to conduct more research on the disturbance mechanism of new double tunnels parallel undercrossing existing tunnels over a short distance. For studying parallel undercrossing, although a model test is the most effective method to reflect the real process, the implementation of a model test is complex, expensive, and time-consuming. The theoretical analysis method has many assumptions. Moreover, it is difficult to solve, or the deviation in analytical results is too large for complex stratum and construction conditions. In contrast, the numerical simulation method is a good alternative to accurately evaluate the construction response (Li et al. [19]).

In this study, combined with the case of Hefei subway tunnel project, a numerical method was used to evaluate the disturbance mechanism of existing tunnel and ground caused by the construction of parallel double tunnels undercrossing over a short distance. The purpose of this study is not only to analyze the effect of parallel undercrossing construction mode on the safety of existing tunnels but also to assist engineers in developing effective construction risk control measures. The study mainly includes the following three parts. First, FLAC^{3D} finite difference software was used to build a 3D numerical model of a new double-line shield tunnel undercrossing the existing tunnel over a short distance in a parallel mode, and the effect of shield tunnel construction process on surface settlement, existing tunnel settlement, and lining internal force was analyzed. Second, the validity of model was verified using field monitoring data. Finally, based on the numerical model, the effects of change in stratum sensitivity on the settlement of existing tunnel, lining internal force, and surface settlement are discussed. In the conclusion and discussion section, the numerical simulation results are combined to analyze the risk control measures of this project.

2. Project Case

2.1. Case Overview. This paper is based on the case study of Hefei subway project in China. The plan view and spatial location of the project are shown in Figure 1. Subway line 1 was completed and put into operation. Subway line 5 is a new metro line. Figure 1(a) shows a planned overlapping area between lines 1 and 5, and the length of overlapping area is approximately 120 m. Figure 1(b) shows the spatial location relationship between lines 1 and 5. The minimum distance between the left and right lines of line 5 is 3.3 m; the minimum buried depth is 17.67 m; the minimum distance

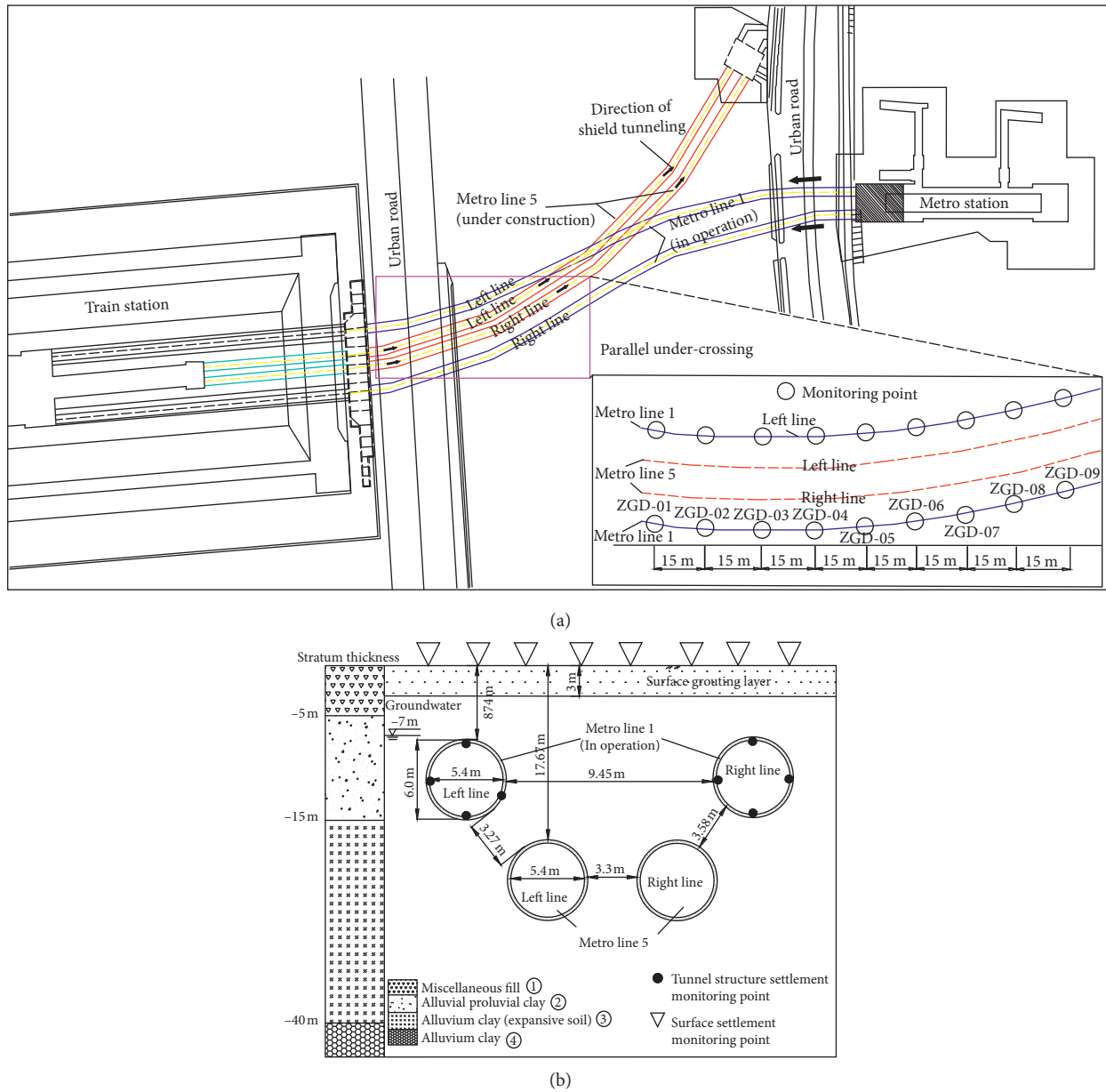


FIGURE 1: Plan and spatial location of subway tunnels of lines 1 and 5. (a) Plan position of tunnel and layout of monitoring points. (b) Spatial location of tunnels.

between the left and right lines of line 1 is 9.45 m; the minimum buried depth is 8.74 m. The minimum clear distance between the left line of line 1 and the left parallel section of line 5 is only 3.27 m, and the minimum clear distance between the right line of line 1 and the right parallel section of line 5 is only 3.58 m. The newly built tunnel uses a slurry-pressure-balance shield machine, which can maintain the safe tunnelling of shield machine by controlling the balance between mud pressure inside the shield machine and the pressure of soil in front of the tunnel.

Combined with the stratum conditions of the project, the grouting method and high-pressure jet mixing method were used to reinforce the stratum within 3 m from the surface to the underground of the project to improve the strength and

impermeability of stratum. C35 grade concrete was used for the lining of existing metro tunnel line 1. To reduce the disturbance to the existing tunnel, high-strength concrete C50 was used to improve the lining stiffness of line 5.

2.2. Regional Stratigraphic Conditions. The stratum distribution and properties from the top to the bottom of the project are described as follows:

The site is covered with Quaternary Holocene artificial miscellaneous fill ①: it is composed of broken bricks and domestic garbage. It is loose and dry and distributed on the surface of site with a thickness of 0.5–5 m.

Alluvial proluvial clay ②: hard plastic, medium compressible soil with a high dry strength and a thickness of 7–12 m.

Upper Pleistocene alluvium clay (expansive soil) ③: hard plastic, medium compressible soil with a high dry strength and a thickness of 20–25 m.

Middle Pleistocene alluvium clay ④: hard plastic, medium compressible soil, high dry strength, and relatively hard with a thickness of 8–12 m.

The test results of physical and mechanical parameters of rock strata in the geological investigation are shown in Table 1, and the values of these parameters are also required for numerical simulation. In addition, the groundwater level in these strata is mainly supplied by atmospheric precipitation, and the buried depth of groundwater level is in the range of 1.5–10.5 m. Therefore, the effect of groundwater on the stratum and tunnel construction should be considered during the simulation.

3. Numerical Simulation Scheme

The FEM, DEM, and FDM are the three main numerical methods to analyze geotechnical engineering problems. In addition, the discontinuity layout optimization numerical method has unique advantages in the study of tunnel structure stability [20, 21], but this study does not involve this aspect. The FEM has obvious advantages in the analysis of geometry, linear solution, phase field model, and the efficiency of dealing with complex problems [22, 23]. The DEM is very suitable for simulating the deformation and failure of discrete particle assemblies under quasistatic or dynamic conditions [24, 25]. However, the FDM seems to be more effective in the solution of deformation problems of geotechnical engineering, which is also the reason for selecting the FDM in this study.

3.1. Calculation Model. FLAC^{3D} finite difference software was used to build the 3D model, as shown in Figure 2. In actual engineering, the two lines are not completely linearly parallel, and the radius of curve is about 1500 m. This study approximated the relationship between the two lines as straight parallel. The length, width, and height of the model are 120 m, 91 m, and 50 m, respectively; the vertical distance between the top of the model and the center point of the tunnel of line 5 is 21 m; the distance between the left and right sides of model and the centerline of line 5 is 40.85 m. To correspond with the actual project, the longitudinal (*Y*-axis direction) length of the model was kept as 120 m. The inner diameter of lining of subway lines 1 and 5 is 5.4 m, and the lining thickness is 0.3 m. Model boundary conditions are as follows: the bottom of the model restricts its displacement in the *Z* direction; the side of the model restricts its displacement in the *X* direction; the surface of the model (*Z* = 51) is the surface, a free boundary.

3.2. Constitutive Model and Parameters. The constitutive model of soil is the Mohr–Coulomb model; the lining of

shield tunnel used a solid linear elastic model; the soil after excavation used a null element simulation. The isotropic seepage model was used in seepage simulation, i.e., the seepage difference in different directions was not considered. During building the calculation model, the physical and mechanical parameters of the soil layer in Table 1 were selected. The cohesion values, internal friction angles, and elastic moduli of materials in the reinforcement area increased by 20% compared with the mechanical parameters of soil materials [26]. The lining parameters of shield tunnel were selected according to the actual values of parameters, and the mechanical parameters of lining are shown in Table 2. Before tunnel excavation, the pore water pressure is hydrostatic pressure. In the seepage model, the four sides and the bottom of the model are impermeable boundaries, and the groundwater level is an impermeable boundary. After tunnel excavation, the pore water pressure of tunnel wall was fixed to zero.

3.3. Simulation Steps. In the construction scheme, the right line of line 5 was first excavated and pushed forward at an average speed of 5 rings per day. After the right line is connected, the left line of line 5 was excavated again to keep the shield driving speed unchanged. The shield excavation length of line 5 is 120 m. The actual amount of excavation in a day during construction is 5–6 rings. In the calculation model, the shield excavation was divided into 32 steps, and each step is 7.5 m. Therefore, the excavation of right line and left line of line 5 includes 16 excavation steps. The tunnel lining was simulated by one-time construction, and the soil mass after excavation was simulated by a null element. In the simulation, it was assumed that the pressure exerted on the excavation face by slurry-pressure-balance shield machine varies linearly with elevation and ground density. The stress at the top of tunnel is usually equal to 50% of the total stress at the invert of tunnel. In the actual construction process, an additional thrust force of about 28 kPa was applied to the excavation face. In this study, the face pressure at the tunnel axis was set as 302 kPa.

3.4. Numerical Monitoring Layout. To obtain the numerical simulation monitoring results, during the construction of line 5, combined with the field monitoring measurement scheme, a monitoring section was arranged every 15 m for the operation of tunnel line 1, and four settlement monitoring points were selected on the tunnel section. The starting position of excavation was selected as the settlement monitoring section for surface settlement. The monitoring layout is shown in Figure 1.

4. Simulation Results

4.1. Reliability Verification of Numerical Model. During construction, it is difficult to obtain the monitoring data of two existing tunnels in operation at the same time. Therefore, the left line of line 1 nearest to the construction line was selected for monitoring in this project. The main monitoring content is the crown settlement of left section line of line 1.

TABLE 1: Physical and mechanical parameters of strata.

Stratum name	Thickness (m)	Soil mass (kN m ³)	Cohesion (kPa)	Internal friction angle (°)	Deformation modulus (MPa)	Poisson's ratio	Permeability coefficient (cm/s)	Porosity
Miscellaneous fill ①	5	16.9	8	9	5	0.35	8×10^{-4}	0.64
Alluvial proluvial clay ②	10	19.6	47.5	12	50	0.32	1.0×10^{-6}	0.58
Alluvium clay (expansive soil) ③	25	19.7	49.5	14	200	0.28	1.2×10^{-6}	0.52
Alluvium clay ④	10	19.7	51.5	13	300	0.22	1.5×10^{-7}	0.43

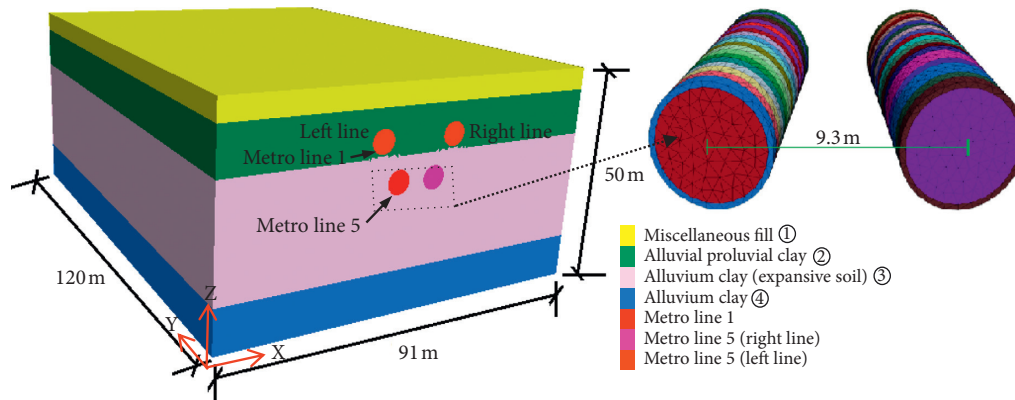


FIGURE 2: Calculation model.

TABLE 2: Shield segment parameters.

Subway tunnel	Lining concrete grade	Modulus of elasticity (GPa)	Poisson's ratio	Density (kg·m ⁻³)	Diameter (m)	Lining ring width (m)	Lining thickness (m)
Line 1	C35	27	0.20	2500	6.0	1.2	0.3
Line 5	C50	35	0.17	2700	6.0	1.5	0.3

The location of field monitoring point is basically the same as that of numerical simulation monitoring point.

After the right line of line 5 starts tunnelling construction, field monitoring was carried out for line 1. The monitoring process is divided into two time periods: the right line and the left line of line 5. The field monitoring data are shown in Figure 3.

Figure 3(a) shows that during the shield construction of right line of line 5, the tunnel settlement of left line of line 1 is obvious, and after the construction of right line of line 5, the maximum vault settlement is 2.2 mm. With the continuous advance of shield construction, the settlement rate of monitoring point near the excavation face was accelerated, and the settlement rate of monitoring point far away from the excavation face slowed down. Figure 3(b) shows that after the construction of right line of line 5, the construction of left line of line 5 significantly affected the settlement of left-line tunnel of line 1. After the construction of left line of line 5, the maximum vault settlement of tunnel of line 1 is 5.32 mm.

In the numerical model, monitoring points were set for the vault of left line of line 1, and the numerical simulation results of vault settlement are shown in Figure 4. By comparing with Figures 3 and 4, it was found that the

development trend of maximum settlement curve of arch crown calculated using FLAC^{3D} is consistent with the change trend of field monitoring results. The comparative analysis results of the maximum settlement and error of the vault obtained from field monitoring and numerical simulation are shown in Table 3. The maximum error between the numerical solution of maximum vault settlement and maximum vault settlement of field monitoring is 6.67%, and the average error is 5.01%. This result shows that the numerical model has considerable reliability and rationality.

4.2. Surface Settlement. The simulation results of surface settlement after tunnel excavation are shown in Figures 5, and 5(a) shows that after the construction of right line of line 5, the maximum value of surface settlement is 2.8 mm, and the maximum point of surface settlement is close to the top of right line of line 5. Figures 5(b) shows that after the construction of double line of line 5, the maximum surface settlement is 3.9 mm, and the maximum point of settlement is close to the top of left line of line 5. The simulation results show that after the completion of double-line tunnel of line 5, the surface settlement is small.

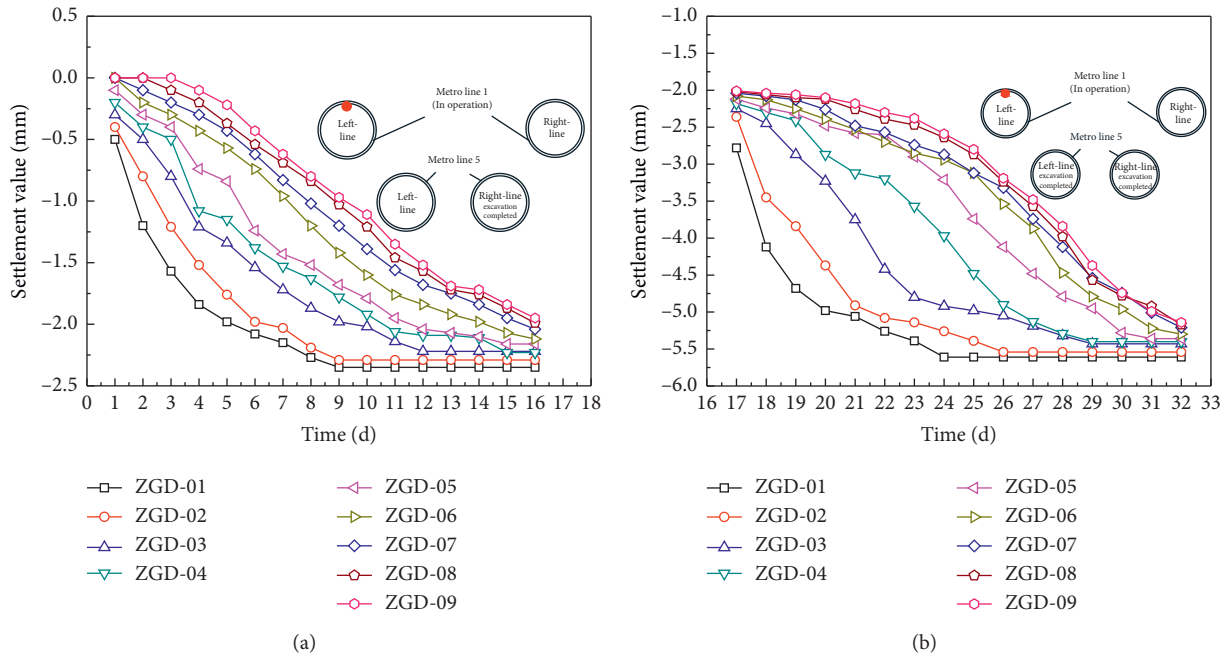


FIGURE 3: Time history curve of tunnel arch crown settlement of left line of line 1 caused by excavation construction of line 5 (field-monitoring results). (a) Right-line tunnelling. (b) Left-line tunnelling.

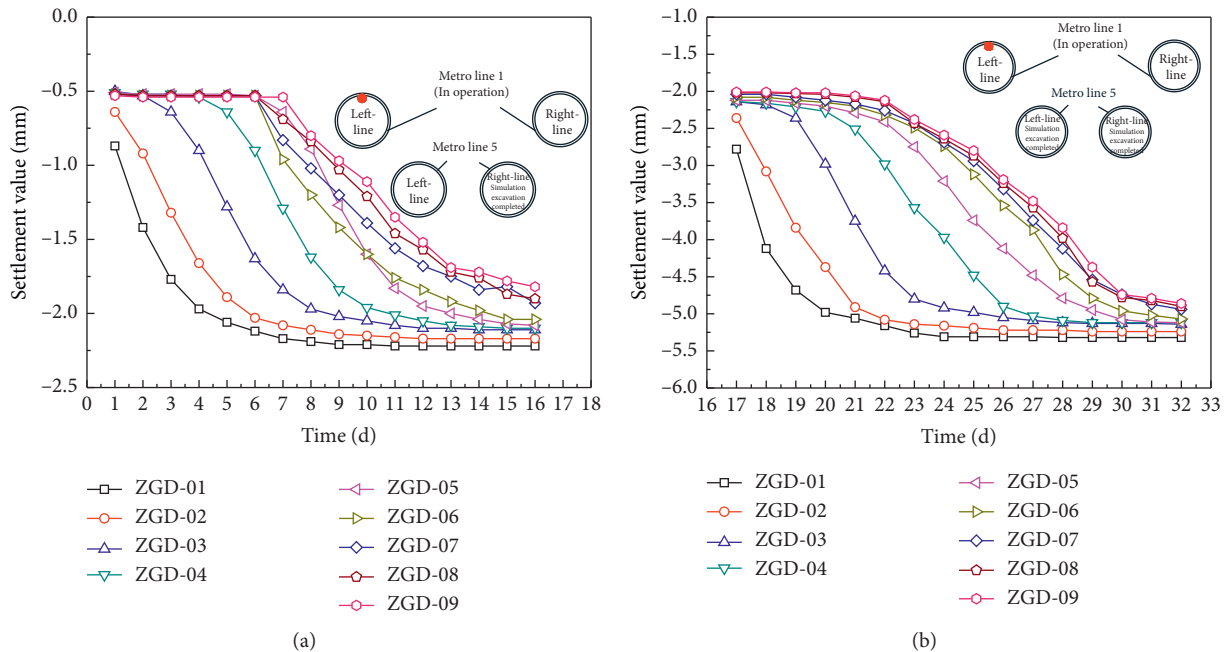


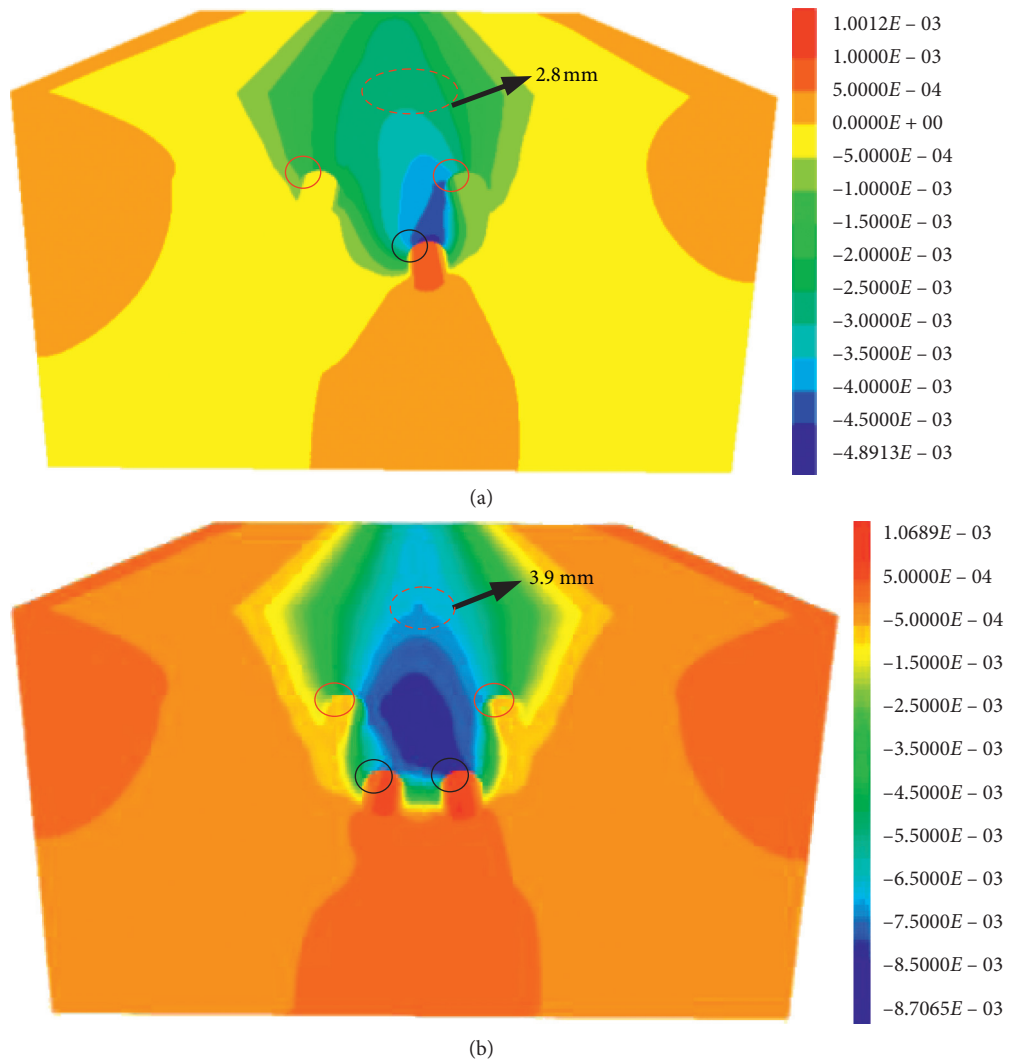
FIGURE 4: Time history curve of tunnel arch crown settlement of left line of line 1 caused by excavation construction of line 5 (numerical results). (a) Right-line tunnelling. (b) Left-line tunnelling.

In addition, from the simulation cloud chart of vertical soil settlement, it was observed that the effect of existing tunnel (metro line 1) on the ground settlement has obvious sheltering effect; the soil settlement above the two sides of existing tunnel is obviously smaller than that of soil in the middle of existing tunnel. The vertical displacement of soil

mass produced by the successive excavation sequence of newly built double-track tunnel (metro line 5) has superposition effect. Therefore, it is necessary to pay special attention to the change and control of soil settlement in the middle of existing tunnel during the sequential excavation of new double-track tunnel.

TABLE 3: The comparative analysis results of the maximum settlement and error of the vault.

Monitoring point number	After excavation of right line of line 5 (numerical results)	After excavation of right line of line 5 (actual value)	Error value (%)	After excavation of left line of line 5 (numerical results)	After excavation of left line of line 5 (actual value)	Error value (%)
ZGD-1	-2.22	-2.35	5.53	-5.32	-5.61	5.17
ZGD-2	-2.17	-2.29	5.24	-5.24	-5.54	5.42
ZGD-3	-2.11	-2.22	4.95	-5.14	-5.43	5.34
ZGD-4	-2.10	-2.23	5.83	-5.12	-5.40	5.19
ZGD-5	-2.08	-2.16	3.70	-5.12	-5.36	4.48
ZGD-6	-2.03	-2.12	4.25	-5.07	-5.30	4.34
ZGD-7	-1.93	-2.04	5.39	-4.94	-5.21	5.18
ZGD-8	-1.90	-1.99	4.52	-4.9	-5.17	5.22
ZGD-9	-1.82	-1.95	6.67	-4.86	-5.14	5.45



FIGURES 5: Simulation results of surface settlement (unit: m). (a) After the construction of right-line tunnel of line 5. (b) After the construction of double-line tunnel of line 5.

4.3. Tunnel Settlement of Line 1. The settlement curve of arch waist and the arch bottom of left and right tunnels of line 1 are shown in Figures 6–8. Figures 6 and 7 show that after the completion of construction of right-line tunnel of line 5, the

settlement of right-line tunnel left arch waist of line 1 is larger than that of left line of line 1. The maximum settlement at the left arch waist of right-line tunnel of line 1 is 4.14 mm, and the maximum settlement difference between

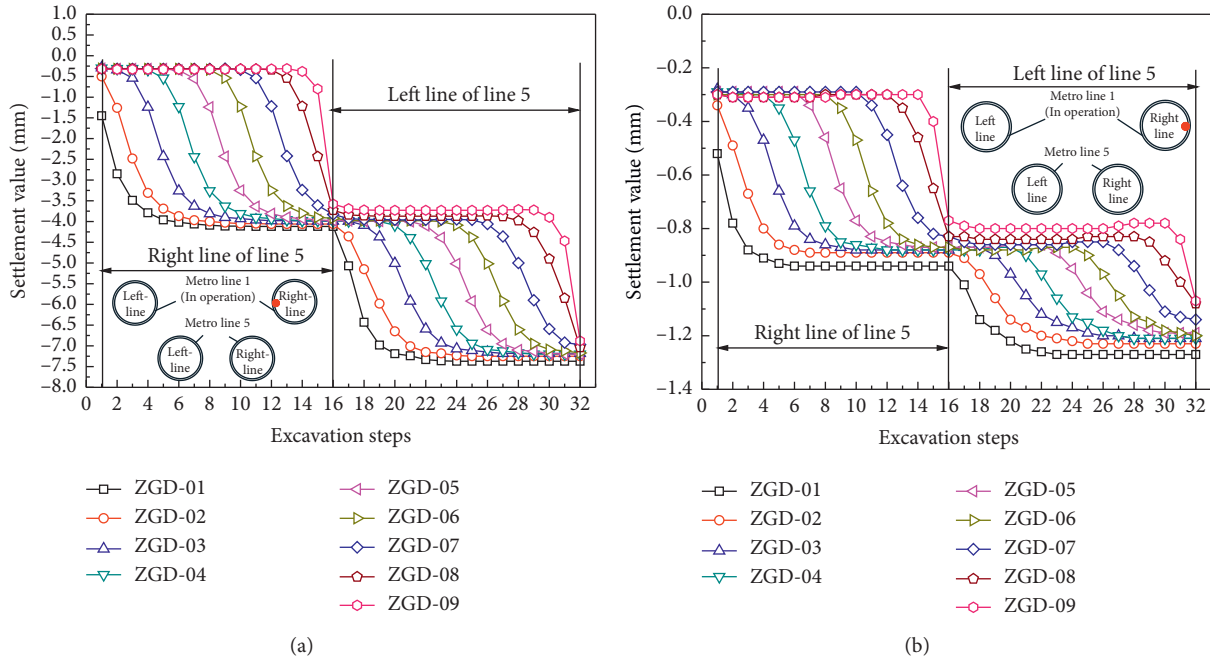


FIGURE 6: Settlement of right-line arch waist of line 1 caused by the construction of line 5. (a) Left-side arch waist. (b) Right-side arch waist.

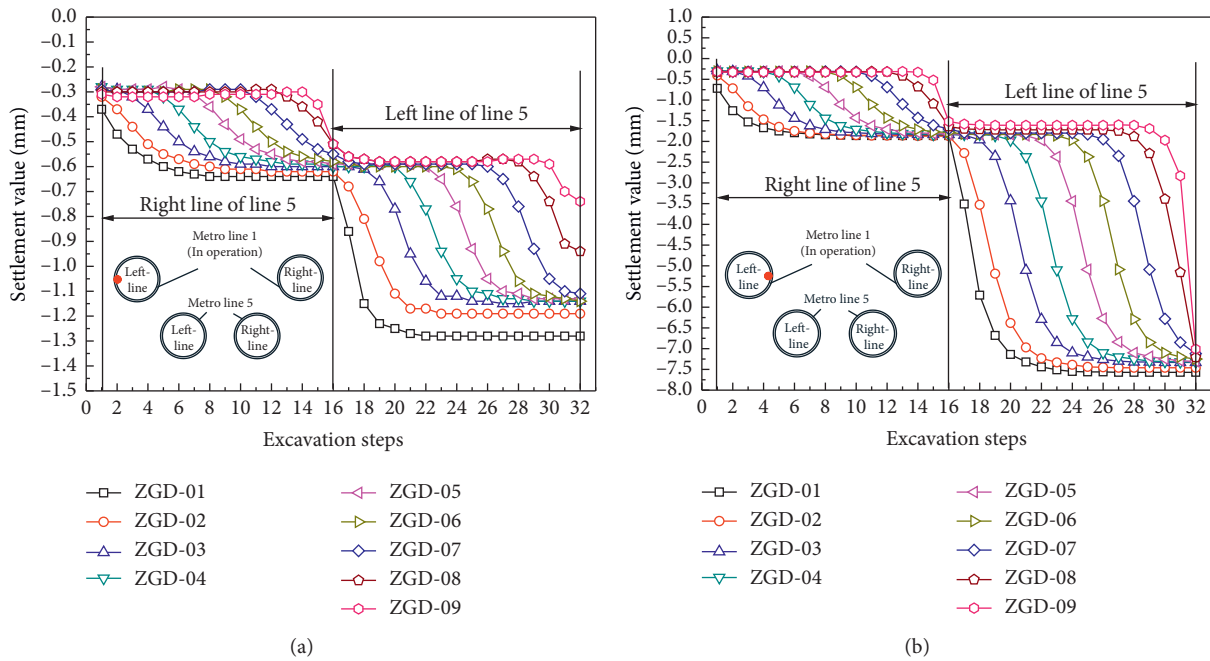


FIGURE 7: Settlement of left-line arch waist of line 1 caused by the construction of line 5. (a) Left-side arch waist. (b) Right-side arch waist.

the left and right arch waist of right-line tunnel of line 1 is 3.12 mm. The maximum settlement of right arch waist of left-line tunnel of line 1 is 2.10 mm, and the maximum settlement difference of left and right arch waist is 1.28 mm. After the construction of left and right double-line tunnels of line 5, the maximum settlement at the left arch waist of right-line tunnel of line 1 is 7.75 mm, and the maximum settlement difference between the left and right arch waist is

6.48 mm. The maximum settlement at the right arch waist of left-line tunnel of line 1 is 7.68 mm, and the maximum difference between the left and right arch waist is 6.40 mm. Figure 8 shows the settlement monitoring curve of arch bottom. The settlement of arch bottom is small, but it is significantly affected by the excavation position.

According to the Technical Code for Protection Structures of Urban Rail Transit (CJJ-T 202-2013), the vertical

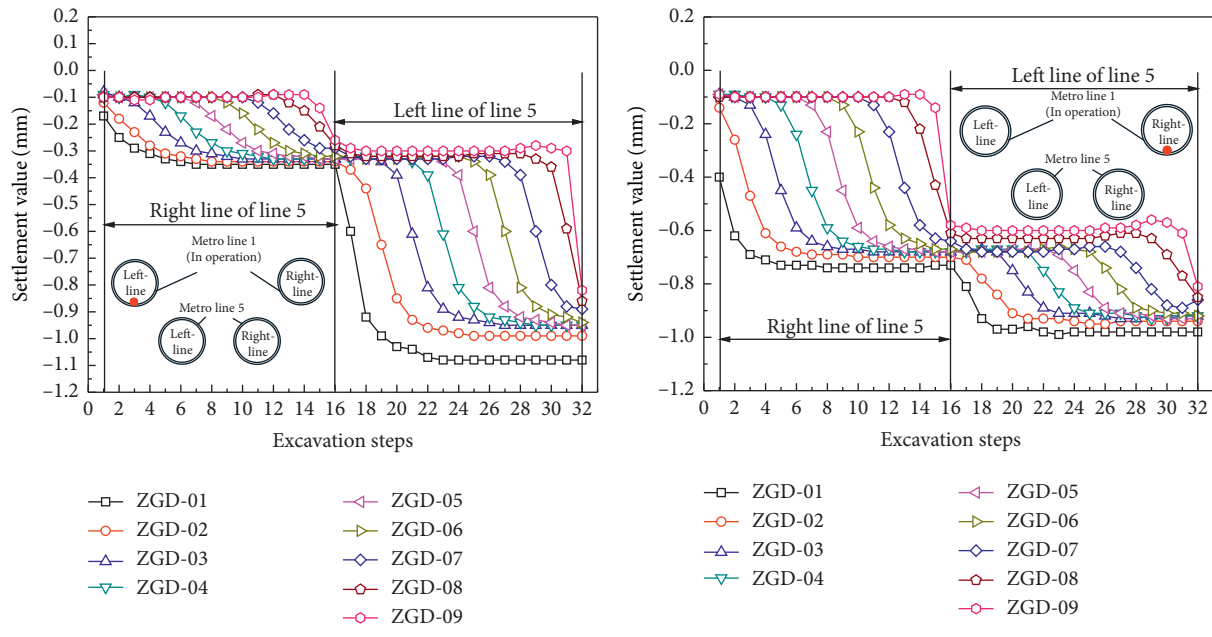


FIGURE 8: Arch bottom settlement of line 1 induced by the construction of line 5. (a) Bottom of left-line arch. (b) Bottom of right-line arch.

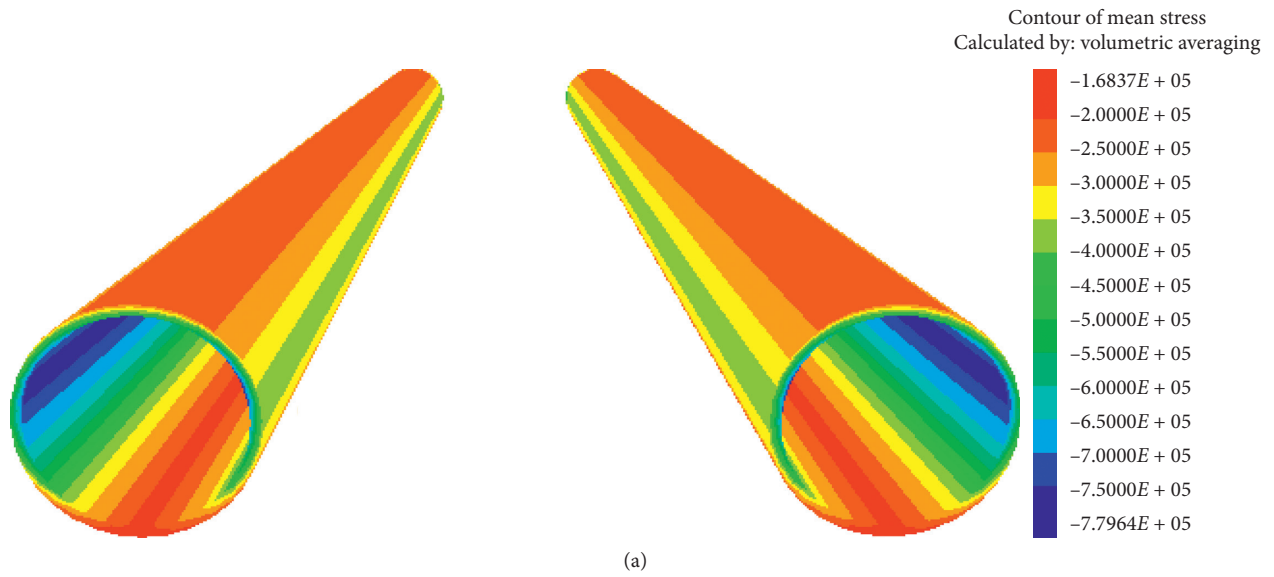


FIGURE 9: Continued.

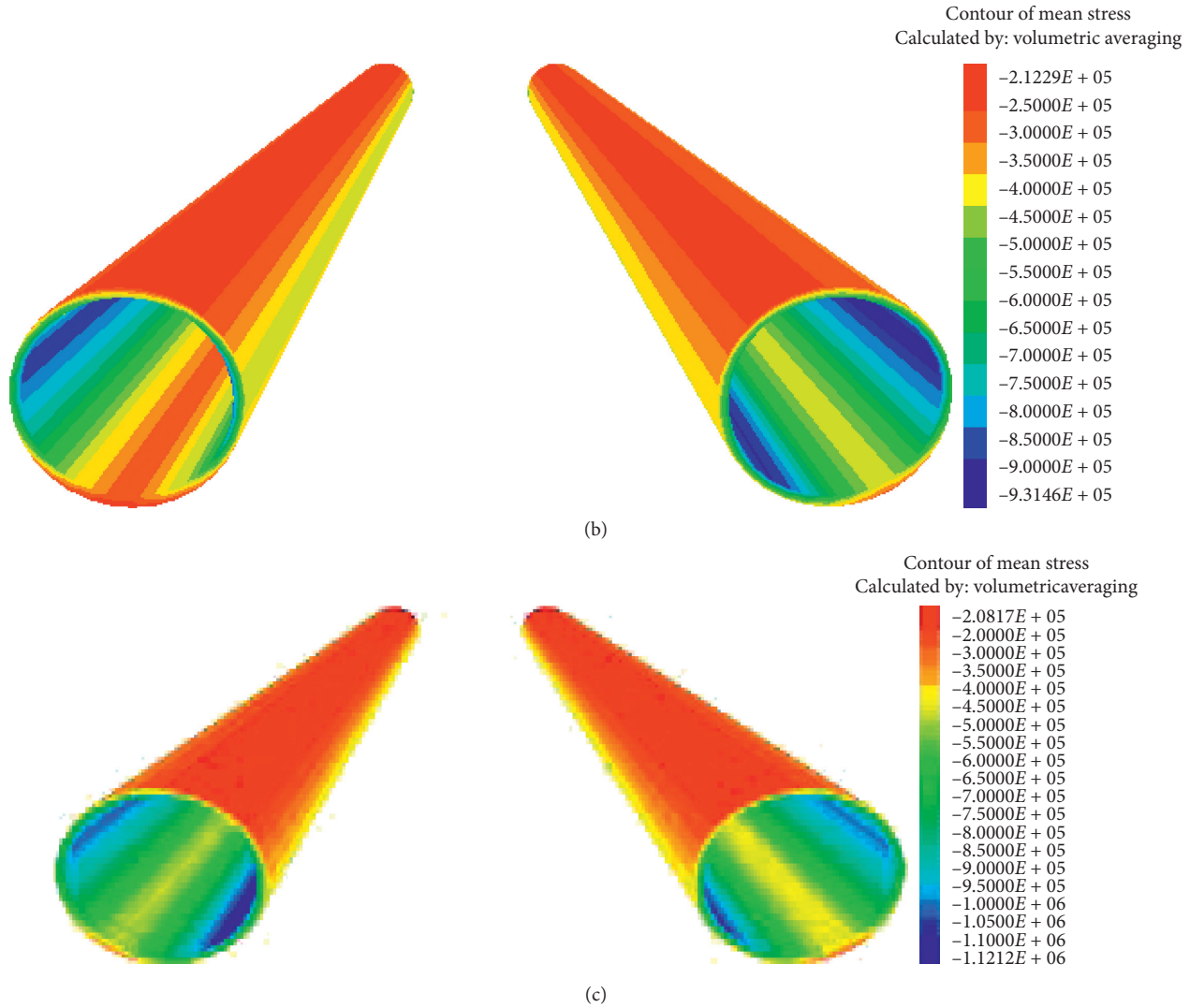


FIGURE 9: Simulation results of lining stress of line 1 (unit: Pa). (a) Line 5 tunnel not constructed. (b) After the construction of right-line tunnel of line 5. (c) After the construction of double-line tunnel of line 5.

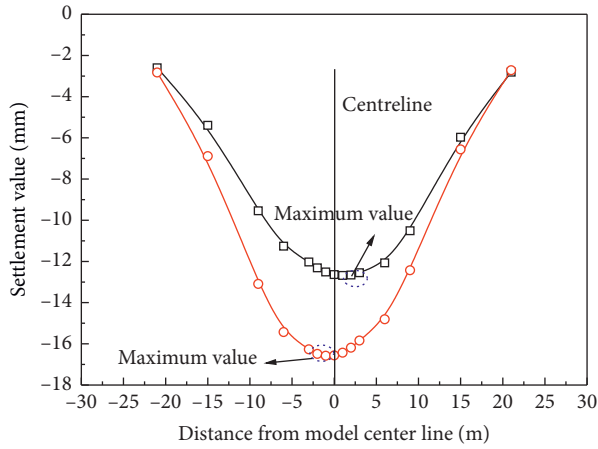
TABLE 4: Strength-weakening scheme of soil layer.

Stratum name	Thickness (m)	Soil mass (kN m ³)	Cohesion (kPa)	Internal friction angle (°)	Deformation modulus (MPa)	Poisson's ratio	Permeability coefficient (cm/s)	Porosity
Miscellaneous fill①	5	16.9	8	9	5	0.35	8.0×10^{-4}	0.64
Miscellaneous fill②	5	16.9	8	9	5	0.35	8.0×10^{-4}	0.64
Miscellaneous fill③	5	16.9	8	9	5	0.35	8.0×10^{-4}	0.64
Alluvium clay④	10	19.7	51.5	13	300	0.22	1.5×10^{-7}	0.43

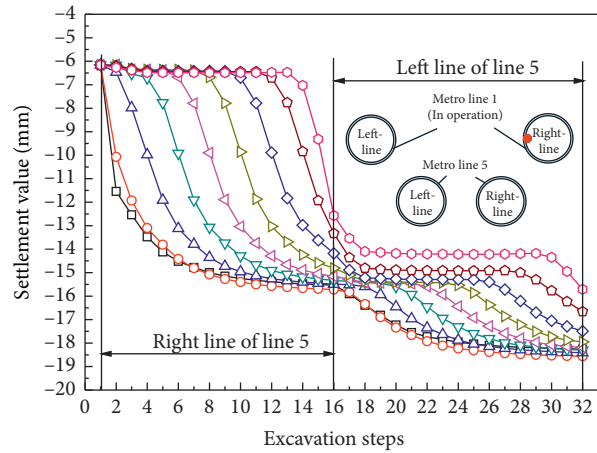
displacement control of tunnel is 20 mm, and the settlement value obtained from numerical simulation of tunnel lining of line 1 satisfies the requirements of code. However, it should be noted that the lining of line 1 shield tunnel is an assembled structure connected by bolts. Excessive differential settlement on both sides of tunnel lining will increase the

internal force of tunnel structure, which might induce structural cracks, concrete crushing, and water leakage.

4.4. Lining Stress of Line 1. Figure 9 shows the simulation results of lining stress of left and right lines of line 1.



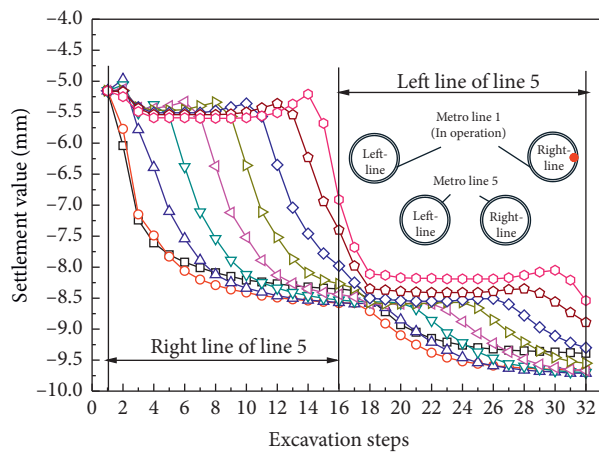
—□— After the construction of right line of line 5
 —○— After the construction of double line of line 5



—□— ZGD-01 ◊ ZGD-05
 —○— ZGD-02 ◊ ZGD-06
 —△— ZGD-03 ◊ ZGD-07
 —▽— ZGD-04 ◊ ZGD-08
 ◊ ZGD-09

(a)

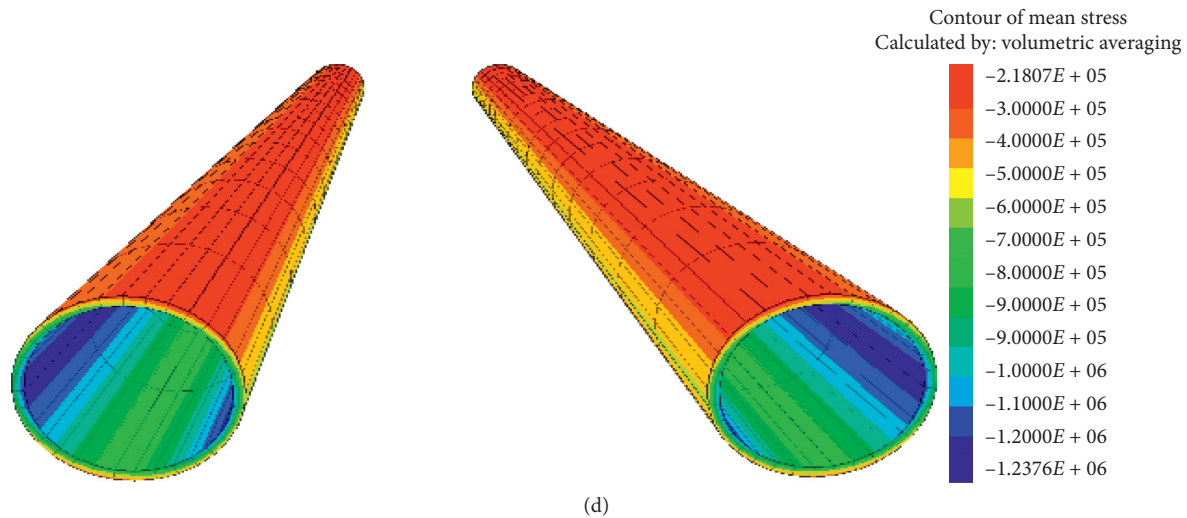
(b)



—□— ZGD-01 ◊ ZGD-05
 —○— ZGD-02 ◊ ZGD-06
 —△— ZGD-03 ◊ ZGD-07
 —▽— ZGD-04 ◊ ZGD-08
 ◊ ZGD-09

(c)

FIGURES 10: Continued.



FIGURES 10: Numerical simulation results after soil layer strength weakening. (a) Surface settlement. (b) Left arch waist settlement of right line of line 1. (c) Right arch waist settlement of right line of line 1. (d) Lining stress of line 1 after the construction of double line of line 5 (unit: Pa).

Figure 9(a) shows that the maximum stress inside the lining of line 1 is 7.798×10^5 Pa when line 5 is not constructed, and the maximum stress is near both sides of arch crown. Figure 9(b) shows that after the construction of right line of line 5, the maximum stress of lining of line 1 is 9.314×10^5 Pa, an increase of 19% than that before the construction. The maximum stress is located near both sides of arch crown, and the stress near the arch bottom of side near line 5 increased most significantly. As the stress increased by 80%, the maximum stress gradually moved toward the arch bottom of one side near line 5. Figure 9(c) shows that after the double-track construction of line 5, the maximum stress inside the lining of line 1 is 1.124×10^6 Pa, 44% higher than that before the construction, and the stress at the vault is 1.036×10^6 Pa, 32% higher than that before the construction. At this time, the maximum stress is near the vault bottom of line 5. Before and after the excavation, the stress position and change in stress size are obvious. It is necessary to strengthen the monitoring of lining stress to prevent damage to the existing subway tunnel lining.

5. Effect of Stratum Change on Disturbance Effect

In some cities in China, metro shield tunnels are built in relatively poor soil conditions and with thick soft soil stratum, such as Shanghai, Shenzhen, and Guangzhou. At the same time, most of these cities have developed subway networks. Therefore, it is necessary to verify whether the above reinforcement measures can ensure the safety of tunnel construction in the case of worse soil conditions. To study the disturbance to the existing subway caused by the parallel undercrossing construction of new tunnel under the condition of a poor soil layer or deep soft soil layer, based on the numerical model constructed in Section 2 of this paper, the thickness of a miscellaneous fill soil layer was increased

to reduce the strength of soil layer. Using the method of stratum strength weakening, the sensitivity changes in surface settlement, existing tunnel settlement, and lining stress due to soil strength weakening were studied, providing a theoretical reference for similar engineering construction and design. In this paper, the scheme of soil layer strength weakening involves a change to the soil layers ② and ③ in Table 1 into a miscellaneous fill, and the parameters are shown in Table 4.

After the soil layer strength is weakened, the simulation results of surface settlement, existing tunnel settlement, and lining stress are shown in Figure 10. By comparing Figures 3 and 10(a), it was observed that after the soil strength is weakened, the maximum surface settlement increased to 17.8 mm, 356% higher than that before the soil strength is weakened. The surface settlement is sensitive to the weakening of soil layer strength.

By comparing Figures 4, 10(b), and 10(c), it was observed that after the strength of soil layer is weakened, the tunnel settlement of line 1 increased significantly, and the maximum settlement appeared at the arch waist of line 1. The maximum settlement is 18.8 mm, and the maximum settlement increased by 142% than that before the weakening. The settlement difference between the left and right sides of arch waist of line 1 reached 10.2 mm, an increase of 59% than that before weakening. This shows that tunnel settlement is very sensitive to changes in soil strength.

Figures 7 and 10(d) show that the effect of stratum weakening on lining stress is not significant, but the initial stress of lining is changed due to tunnel excavation.

6. Conclusions and Discussion

- (1) In this case, during the construction of a parallel undercrossing of an existing tunnel, a large settlement exists at the position of existing tunnel arch waist, and the settlement difference between the two

sides of arch waist is large. Therefore, it is necessary to strengthen the monitoring of position of existing tunnel arch waist to prevent excessive settlement or settlement difference. If necessary, the soil layer should be grouted and reinforced in advance.

- (2) During a parallel underpass construction, the stress of existing tunnel lining is significantly affected, and the maximum stress of lining increased by 80%. To protect the operational safety of existing tunnel, the stress of existing tunnel lining should be monitored to prevent structural cracks caused by the excessive stress change in the existing tunnel lining.
- (3) After the strength of soil layer is weakened, the settlement of existing tunnel increases significantly. For a short-distance parallel shield construction project in an area with poor stratum conditions and deep soft strata, it is necessary to reinforce the strata and strengthen the monitoring of surface settlement to prevent damage to the existing buildings. During shield tunnelling, simultaneous grouting is used to reduce the disturbance to existing tunnel and surface.
- (4) A 3D numerical model of shield tunnelling undercrossing the existing tunnel was developed in this study. The simulation results are highly consistent with the field monitoring data. This shows that the numerical model and related parameters are reasonable and reliable. This study provides valuable information for the safe implementation of a project.

Data Availability

All data are included in the paper.

Conflicts of Interest

The authors declare that there are no conflicts of interest.

Acknowledgments

This work was supported by the National Science Foundation of China (grant nos. 51978668, 51968005, 51538009, 51608537, and 51678166) and the Guangxi University Young and Middle-Aged Teachers' Basic Scientific Research Ability Improvement Project (2020ky01011).

References

- [1] Z. Huang, H. Fu, W. Chen, J. Zhang, and H. Huang, "Damage detection and quantitative analysis of shield tunnel structure," *Automation in Construction*, vol. 94, pp. 303–316, 2018.
- [2] R. Liang, T. Xia, Y. Hong, and F. Yu, "Effects of above-crossing tunnelling on the existing shield tunnels," *Tunnelling and Underground Space Technology*, vol. 58, pp. 159–176, 2016.
- [3] M. Zhang, J. Fan, and B. Y. Pan, "Analysis on construction influence of the underpass of oblique crossing subway tunnel," *Applied Mechanics and Materials*, vol. 6, pp. 716–717, 2014.
- [4] H. Lai, X. Zhao, Z. Kang, and R. Chen, "A new method for predicting ground settlement caused by twin-tunneling under-crossing an existing tunnel," *Environmental Earth Science*, vol. 76, no. 21, p. 726, 2017.
- [5] J. Fu, J. Yang, X. Zhang, H. Klapperich, and S. M. Abbas, "Response of the ground and adjacent buildings due to tunnelling in completely weathered granitic soil," *Tunnelling and Underground Space Technology*, vol. 43, pp. 377–388, 2014.
- [6] D. Zhang, Q. Fang, Y. Hou, P. Li, and L. N. Yuen Wong, "Protection of buildings against damages as a result of adjacent large-span tunneling in shallowly buried soft ground," *Journal of Geotechnical and Geoenvironmental Engineering*, vol. 139, no. 6, pp. 903–913, 2013.
- [7] Z. Zhu, S. Huang, and Y. Zhu, "Study of road surface settlement rule and controlled criterion for railway tunnel undercrossing highway," *Rock and Soil Mechanics*, vol. 33, no. 2, pp. 558–656, 2012.
- [8] S. Ma, Y. Shao, Y. Liu, J. Jiang, and X. Fan, "Responses of pipeline to side-by-side twin tunnelling at different depths: 3D centrifuge tests and numerical modelling," *Tunnelling and Underground Space Technology*, vol. 66, pp. 157–173, 2017.
- [9] C. W. W. Ng, H. Lu, and S. Y. Peng, "Three-dimensional centrifuge modelling of the effects of twin tunnelling on an existing pile," *Tunnelling and Underground Space Technology*, vol. 35, pp. 189–199, 2013.
- [10] J. Shi, Y. Wang, and C. W. W. Ng, "Three-dimensional centrifuge modeling of ground and pipeline response to tunnel excavation," *Journal of Geotechnical and Geoenvironmental Engineering*, vol. 142, no. 11, Article ID 040160543, 2016.
- [11] Z. Wang, K.-W. Zhang, G. Wei, B. Li, Q. Li, and W.-J. Yao, "Field measurement analysis of the influence of double shield tunnel construction on reinforced bridge," *Tunnelling and Underground Space Technology*, vol. 81, pp. 252–264, 2018.
- [12] Q. Fang, D. Zhang, Q. Li, and L. N. Y. Wong, "Effects of twin tunnels construction beneath existing shield-driven twin tunnels," *Tunnelling and Underground Space Technology*, vol. 45, pp. 128–137, 2015.
- [13] R.-P. Chen, X.-T. Lin, X. Kang et al., "Deformation and stress characteristics of existing twin tunnels induced by close-distance EPBS under-crossing," *Tunnelling and Underground Space Technology*, vol. 82, pp. 468–481, 2018.
- [14] G. W. Byun, D. G. Kim, and S. D. Lee, "Behavior of the ground in rectangularly crossed area due to tunnel excavation under the existing tunnel," *Tunnelling and Underground Space Technology*, vol. 21, no. 3-4, p. 361, 2006.
- [15] Z. Zhang and M. Huang, "Geotechnical influence on existing subway tunnels induced by multiline tunneling in shanghai soft soil," *Computers and Geotechnics*, vol. 56, pp. 121–132, 2014.
- [16] X.-T. Lin, R.-P. Chen, H.-N. Wu, and H.-Z. Cheng, "Deformation behaviors of existing tunnels caused by shield tunneling undercrossing with oblique angle," *Tunnelling and Underground Space Technology*, vol. 89, pp. 78–90, 2019.
- [17] C. W. W. Ng, K. Y. Fong, and H. L. Liu, "The effects of existing horseshoe-shaped tunnel sizes on circular crossing tunnel interactions: three-dimensional numerical analyses," *Tunnelling and Underground Space Technology*, vol. 77, pp. 68–79, 2018.
- [18] M. Yin, H. Jiang, Y. Jiang, Z. Sun, and Q. Wu, "Effect of the excavation clearance of an under-crossing shield tunnel on existing shield tunnels," *Tunnelling and Underground Space Technology*, vol. 78, pp. 245–258, 2018.

- [19] Z. Li, J. Chen, M. Sugimoto, and H. Ge, "Numerical simulation model of artificial ground freezing for tunneling under seepage flow conditions," *Tunnelling and Underground Space Technology*, vol. 92, Article ID 103035, 2019.
- [20] Z. Sun, Y. Zhang, Y. Yuan, and H. A. Mang, "Stability analysis of a fire-loaded shallow tunnel by means of a thermo-hydro-chemo-mechanical model and discontinuity layout optimization," *International Journal for Numerical and Analytical Methods in Geomechanics*, vol. 43, no. 16, pp. 2551–2564, 2019.
- [21] Y. Zhang, X. Zhuang, and R. Lackner, "Stability analysis of shotcrete supported crown of NATM tunnels with discontinuity layout optimization," *International Journal for Numerical and Analytical Methods in Geomechanics*, vol. 42, no. 11, pp. 1199–1216, 2018.
- [22] S. Zhou, X. Zhuang, and T. Rabczuk, "Phase-field modeling of fluid-driven dynamic cracking in porous media," *Computer Methods in Applied Mechanics and Engineering*, vol. 350, pp. 169–198, 2019.
- [23] X. Zhuang, S. Zhou, M. Sheng, and G. Li, "On the hydraulic fracturing in naturally-layered porous media using the phase field method," *Engineering Geology*, vol. 266, Article ID 105306, 2020.
- [24] E. V. Shilko, S. G. Psakhie, S. Schmauder, V. L. Popov, S. V. Astafurov, and A. Y. Smolin, "Overcoming the limitations of distinct element method for multiscale modeling of materials with multimodal internal structure," *Computational Materials Science*, vol. 102, pp. 267–285, 2015.
- [25] L. Sun, C. Zhou, D. Qin, and L. Fan, "Application of extended distinct element method with lattice model to collapse analysis of RC bridges," *Earthquake Engineering & Structural Dynamics*, vol. 32, no. 8, pp. 1217–1236, 2003.
- [26] C. P. Zhang, Yi Cai, and W. Zhu, "Numerical study and field monitoring of the ground deformation induced by large slurry shield tunnelling in sandy cobble ground," *Advances in Civil Engineering*, vol. 2019, Article ID 4145721, 2019.